JJMIE

Volume 9 Number 2, April.2015
ISSN 1995-6665
Pages 139 - 147

Jordan Journal of Mechanical and Industrial Engineering

Computational Modeling of Temperature Field and Heat Transfer Analysis for the Piston of Diesel Engine with and without Air Cavity

Subodh Kumar Sharma[* a], Parveen Kumar Saini[b], Narendra Kumar Samria[c]

[a]Research scholar, Department of Mechanical Engineering, National Institute of Technology Kurukshetra, Kurukshetra, INDIA
[b]Assistant Professor, Department of Mechanical Engineering, National Institute of Technology Kurukshetra, Kurukshetra, INDIA
[c] professor, Department of Mechanical Engineering, Banaras Hindu University, Varanasi, INDIA

Received 28 Jun 2014 *Accepted 24 April 2015*

Abstract

The present paper presents a theoretical study carried out to investigate the temperature field and heat transfer rate from the pistons of diesel engines with and without air cavity. The material was removed inside the piston, creating an air cavity. This cavity acts as an insulating medium which prevents the heat flow; thus, the need for providing insulation coating on piston crown is minimized. The main motive of this is to reduce the weight of the engine and the cost associated with thermal barrier coating. A detailed analysis was given for estimating the heat transfer rates to the cooling media and temperature field (isothermal distribution) in the piston body of water-cooled engines at different loads with and without air cavity. This analysis was done with numerical simulation models using FORTRAN programming. Results indicate that after creating an optimized air cavity in the piston, temperature, at all nodal point, decreases, which was presented in the form of contour bands and 4% of reduction in heat loss through piston, which leads to a better thermal efficiency. The FEA result provides effective theoretical evidence for further improving the pistons' performance. Additional benefits include protection of metal combustion chamber components from thermal stresses and reduced cooling requirements.

Keywords: *Combustion Chamber, Piston, Temperatures, Diesel Engine Components Temperature Field, Finite Elements.*

Nomenclature

K_x, K_y, K_z	:Thermal conductivity in X, Y and Z direction respectively (W/m.K)
q_E	: Heat conduction per unit volume (J/m^3)
ρ	: Density of the material (kg m^{-3})
$A^{(e)}$	: Area of the Element (e) (m^2)
$V^{(e)}$	: Volume of the Element (e) (m^3)
C	: Specific Heat (W.Kg^{-1}.K$^{-1)}$
$Ø$	: Engine crank angle (^{o}CA)
e	: Element Number (e)
E	: Young's Modulus of Elasticity (N.m^{-2})
i, j, k	: Nodal Point Number of an element
q_g	: Heat Generation per Unit Volume (J.m^{-3})
r_m	: Mean radius (m)
r_{ij}	: Difference Between r Co-ordinates of Nodal Point i & j
s_{ij}	: Distance between Nodal Points i & j
N_s	: Shape factor
T	: Temperature Variable (K)
T_α	: Surrounding Temperature (K)
T_s	: Surface Temperature (K)
H_c	: Convective heat transfer coefficient (W.m^{-2}.K^{-1})
χ	: Variational Integral
χ_b	: Boundary Term of Variational Integral
$\chi_{bconv.}$	: Variational Integral for convective boundary
$\chi_{bcont.}$	: Variational Integral for contact boundary
$\chi_k^{(e)}$	: Conductive matrix
$[k]^{(e)}$	: Stiffness matrix
$\{t\}^{(g)}$	: Global temperature

1. Introduction

The present scenario of the energy crisis and the increasing requirement of internal combustion engines with heavy loads has made it necessary to find new ways of using petroleum fuel more efficiently in the internal combustion engine. To obtain high efficiency, fuel energy

* Corresponding author. e-mail: subodh_meet@yahoo.com.

is not to be wasted due to heat losses through combustion chamber components. One of the most changeling components for analysis is the piston due to its reciprocating motion. In the diesel engine, almost 30% of the fuel energy is wasted due to heat losses through combustion chamber components [1]. For an optimum design consideration of internal combustion engine, the knowledge of heat transfer rate from the working gases to the piston and from the wall of combustion chamber is of great importance. Heat transfer affects the thermodynamic performance of the engine and the result in thermal loading imposes a limit on the engine rating. For that reason, knowledge of the heat transfer in internal combustion engines is important to understand such systems [1, 2]. In addition, it is essential for the assurance of the stability of the engine components to avoid engine body distortions and to improve the engine design related to weight and auxiliary energy consumption. In the case of the engine piston, such knowledge is necessary to have a thorough understanding of heat flux, temperature and the distribution of these parameters. Engine heat transfer phenomena have been broadly analyzed for many decades [3-8]. Numerous mathematical models have been proposed including correlations based on dimensional analysis, which are widely accepted [7, 8]. In addition, Computational Fluid Dynamics (CFD) and/or Finite Element Method (FEM) codes, used for heat transfer simulations, require the assessment of this temperature to provide boundary conditions where convergence is attained through an iterative process [9, 10]. Furthermore, thermal analyses require the gas-side wall temperature to calculate temperature distribution and the thermo-mechanical behavior of components [11, 12]. Thermodynamic analysis of spark ignition engines is introduced by implementing temperature dependent specific heats [13, 19, 22]; it is found that the constant specific heat models can only be used for very small temperature variations so far large changes in temperature, variable specific heat models should be implemented. Understanding the temperature field in parts of internal combustion engine is most important in order to discover the points of highest thermal stress [14-18]. Further, a finite element model of gasoline spark engine was successfully developed and simulated and analyzed heat transfer during the combustion process, obtaining temperature distribution across the major engine component [20]. Temperature and the thermal stress field of the convention and ceramic coated piston of diesel engine were investigated by using the wavelet finite-element method, ANSYS software [21]. In addition, ceramic-coated pistons are being widely used in the internal combustion engine to improve the performance of the engine. This coating works as an insulating layer that reduces heat losses of the internal combustion engine and obtains higher efficiency. For a better performance and stress distribution over the whole combustion chamber components, the optimum coating thickness is found to be near 1 mm. It was also found that, with increasing the thickness of the coating, top surface temperature of the piston increased in a decreasing rate [22, 23]. During thermal cycling from room temperature to 1150°C, the thermal conductivity and diffusivity of TBC coating increase [24]. Other studies showed the effect of thermal barrier coatings on diesel engine performance of PZT loaded cyanate modified epoxy coated combustion chamber [25]. For instance, pistons are very important component in a diesel engine blast chamber due to their operational conditions. To improve the engine performance, most of the studies focused on heat transfer analysis with thermal barrier coated piston [26-29]. A new trend in the field of the internal combustion engine has been taken to make it adiabatic by creating an air cavity inside all the parts like cylinder wall, cylinder head and engine valves. By creating an air cavity inside the engine piston, the weight and cost associated with Thermal Barrier Coating (TBC) are minimized.

The specific objective of this paper is to predict the temperature field developed and the heat transfer rate through the diesel engine piston, considering the spatial variation of heat fluxes with and without the air-cavity and compare the behavior of the conventional (without air cavity) piston and piston with air cavity under thermal loading conditions. This approach is based on energy balances theory.

2. Statement of the Problem

Due to the depletion of energy at a tremendous rate, the present paper investigates the employing of air cavity inside the piston, which was found to be a good functional solution for the imminent lack of energy. So, this investigation is concerned with temperature distribution and heat transfer analysis in the piston (with and without air cavity) of the AV1 diesel engine, as shown in Figure 1. The engine is a single cylinder engine. The compression ratios and, consequently, the power and the torque are different. Selected technical data for the AV1 engine are provided in Table 1. The piston diameter is 75 mm and depth is 72 mm while the thickness of cavity in the piston is 4 mm and the height is 10 mm. The thickness of the piston ring is 10 mm. The thermo physical materials properties and heat transfer parameter for four different cases of engine loading of the piston are given in Tables 2 and 3. In Table 3, T and H represent the temperature and heat transfer coefficient; subscripts g, w and a represent the boundaries of the piston on the gas side (combustion chamber), water jacket side, and air side (crank case). Using the governing equation and the appropriate boundary conditions, the mathematical variational statement of the problem was obtained and then a 2-dimensional finite element model was formulated. With the help of these boundary conditions and finite element technique, temperature distribution and heat transfer analysis over the piston were analyzed by using FORTRAN programming. Figure 2 represents the meshed piston model with all the boundaries conditions.

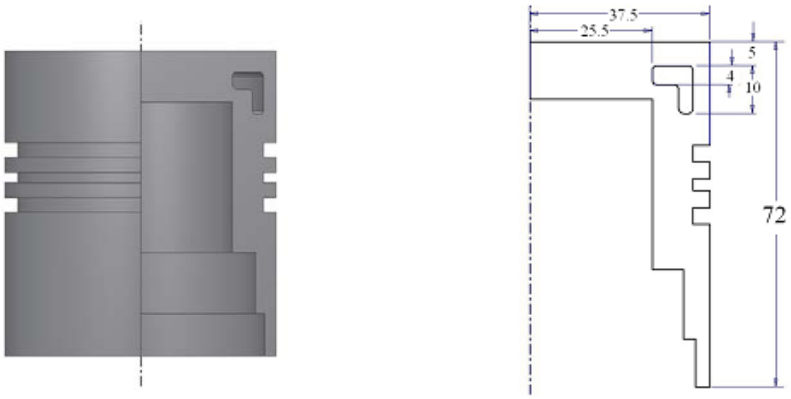

Figure 1. Model of Diesel Engine Piston

Table 1. Engine and their specification [26]

Specification	Type	Specification	Type
Cooling	Water-Cooled Engine	Governing	Class"B1"
Model	AV1	Power rating	5 hp
No. of Cylinders	1	Fuel injection	Direct Injection
Cubic Capacity (ltr)	0.553	Rated Speed (rpm)	1500
Overall Dimensions of the standard engine		617 X 504 X 843 (L X B X H)	

Table 2. Thermo physical properties of metal [26]

Sr. No.	Properties	Aluminium	Cast iron	Steel
1	Thermal conductivity ($W.m^{-1}.K^{-1}$)	175	70	50
2	Density ($Kg.m^{-3}$)	2700	7200	7850
3	Thermal diffusivity ($m^2.hr^{-1}$)	0.259	0.04563	0.044
4	Specific Heat ($KJ.Kg^{-1}.K^{-1}$)	0.8958	0.5860	0.4730

3. Boundary Condition at the Combustion Chamber Components

One of the most fundamental factors in temperature prediction at the combustion chamber components is the correct application of boundary conditions. This involves the ambient temperature and heat transfer coefficients at the various areas of the above components. The instantaneous values of heat transfer coefficient (h_g) and temperature (t_g) at combustion gas side is a function of crank angle (Ø) [2, 3, 5, 11, 17, 18]. Afterwards, the mean value of the heat transfer coefficient H_g and the resulting gas temperature T_g over the complete four-stroke engine cycle are calculated from the formulae given in Ref. [9,18] as:

$$Hg = \frac{1}{Ø0}\int_0^{Ø0} hg(Ø)dØ \quad (1)$$

$$Tg = \frac{\int_0^{Ø0} hg(Ø)\mathrm{tg}(Ø)\mathrm{d}Ø}{\int_0^{Ø0} hg(Ø)\mathrm{d}Ø} \quad (2)$$

In the present study, the following correlation, which was obtained by using the formula given by Eichelberg [9, 18], was used to predict instantaneous heat transfer coefficients. The instantaneous value of heat transfer coefficient h_g (Ø) on the gaseous face at any crank angle (Ø) is obtained from the pressure-crank angle diagram as:

$$h_g(Ø) = 7.64(S)^{1.5}[P_g(Ø)\,T_g(Ø)]^{0.5}\ (W\,m^{-2}K^{-1}) \quad (3)$$

where
P_g (ϕ) is gas pressure (N/m^2)
T_g (ϕ) is gas temperature ($^{\circ}C$)
S is mean piston speed (m/s)

In the thermal analysis, cycle averaged values of combustion heat transfer coefficient and combustion temperature were used for piston top. Temperature and heat transfer coefficient boundary conditions, for all the parts of the piston, were determined based on the authors' experience and on literature [18]. The thermal boundary conditions consist of applying a convection heat transfer coefficient and the bulk temperature, and they are applied to the piston crown, piston ring land sides, piston ring groove lands, and piston under crown surfaces. The temperature and heat transfer coefficients, in the

combustion chamber in all the loading condition, were identified based on data provided in a previous research paper [13, 26]; they are presented in Table 3.The adopted heat transfer coefficient on the contact surfaces are H_a (heat transfer coefficient at piston under crown surface) = 174.3 w/m^{2}k, *H1* (heat transfer coefficient at ring lands and piston skirt upper and lower side) = 290.54w/m^{2}k, *H2* (heat transfer coefficient at ring lands and piston skirt contact surfaces) = 20 w/m^{2}k, *H3* (heat transfer coefficient between piston rings and cylinder wall contact surfaces) = 38346 w/m^{2}k, *H4* (heat transfer coefficient between piston and cylinder wall contact surfaces) = 2324w/m^{2}k, H_w (heat transfer coefficient through cylinder wall to water) = 1859.2w/m^{2}k, and temperature on water side (T_w) was 120°C and on crank case side (T_a) it was 80°C.

4. Finite Element Formulation of Heat Transfer Equations

The variational method constitutes a powerful approach to the formulation of an element relationship. In the theory of finite element analysis, first, the proper variational principle is selected and, then, the function involved is expressed in terms of approximate assumed displacements, which satisfies the given boundary conditions. Then, by minimizing the approximate function, a set of governing equations is developed for the whole piston body. Computer algorithm and FORTRAN program code are developed to solve these equations in order to find the unknown parameters, i.e., the temperature and the heat flow rate.

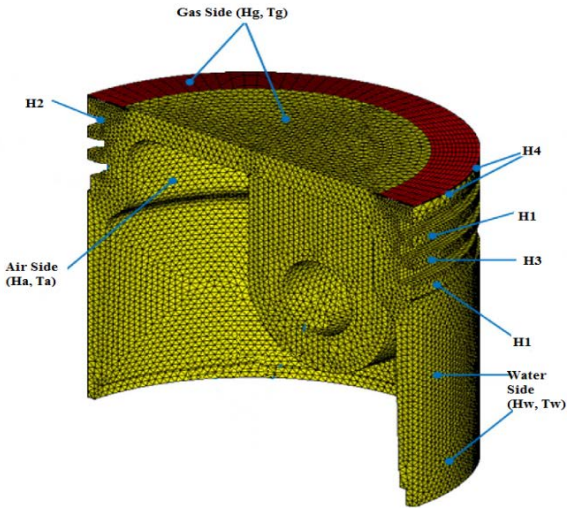

Figure 2. Meshed view of Piston Model

4.1. Heat Transfer Equation for Conduction

The generalized governing differential equation for heat conduction can be represented as [1, 4]:

$$K\nabla^2 T + q_E - \rho C\frac{\partial T}{\partial t} = 0 \qquad (4)$$

where,

K – Thermal conductivity in X, Y and Z direction, respectively

q_E – Heat conduction per unit volume

ρ – Density of the material

C – Heat transfer capacity of the material

And in cylindrical co-ordinates, three dimensional generalized governing differential equations for heat conduction with considering steady state and no internal heat generation can be represented as, Eq. (4) which can be written as:

$$\nabla^2 T = \frac{\partial^2 T}{\partial r^2} + \frac{1}{r}\left(\frac{\partial T}{\partial r}\right) + \frac{1}{r}\left(\frac{\partial^2 T}{\partial \theta^2}\right) + \frac{\partial^2 T}{\partial Z^2} = 0 \qquad (5)$$

Let us consider that there are "*N*" numbers of nodal points having temperature t_1, t_2, t_3 …..t_n whose values are to be determined by the finite element method. Here the principle of minimization is used in order to get the unknown temperatures. First, the variation integrals are differentiated with respect to the corresponding nodal points and equated to zero to yield the temperature at that point. Let us consider a triangular element having nodes *i, j, k* in anticlockwise direction. Assuming a linear polynomial equation of temperature can be represented as;

$$t^e = c_1 + c_2 r + c_3 z$$

Let t_1, t_2, t_3 and $(r_i, z_i), (r_j, z_j), (r_k, z_k)$ be the temperature and (r, z) co-ordinates of an element having nodes *i, j, k* , respectively.

The variational integral in axis symmetric co-ordinate system for heat conduction can be represented as:

$$\chi_K^{(e)} = \frac{1}{2}(2\pi K)\iint_A \left[\left[\frac{\partial t}{\partial r}\right]^2 + \left[\frac{\partial t}{\partial z}\right]^2\right] r dr dz \qquad (6)$$

Here a linear polynomial is chosen to approximate the variation of temperature within an element in terms of the temperature at the nodal points of the elements. Polynomials are chosen in such a way that maintains continuity along the element boundaries. The shape function N_i, N_j and N_k are chosen for a particular element according to variations of the parameters within the elements. The Polynomial, chosen in terms of shape function, is given by in Eq. (7):

$$t(r,z) = [N_I \quad N_J \quad N_K]\begin{Bmatrix} t_i \\ t_j \\ t_k \end{Bmatrix} = [N]^{(e)}\{t\}^{(e)} \qquad (7)$$

where the constants are

$$N_i = \frac{[a_i + b_i r + c_i z]}{\Delta} \quad ; N_j = \frac{[a_j + b_j r + c_j z]}{\Delta};$$

$$N_k = \frac{[a_k + b_k r + c_k z]}{\Delta}$$

$$a_i = (r_j z_k - z_j r_k),\ a_j = (r_k z_i - z_k r_i),$$

$$a_k = (r_i z_j - z_j r_i),$$

$$b_i = (z_j - z_k),\quad b_j = (z_k - z_i),\quad b_k = (z_j - z_i),$$

$$c_i = (r_k - r_j),\quad c_j = (r_i - r_k),\quad c_k = (r_j - r_i)$$

Differentiating the above equation (7) with respect to co-ordinates (*r*, *z*), which is shown in equation (8):

$$\frac{\partial t^{(e)}}{\partial r} = [b_i \quad b_j \quad b_k]\{t\}^{(e)} = [b]^{(e)}\{t\}^{(e)}$$

$$\frac{\partial t^{(e)}}{\partial z} = [c_i \quad c_j \quad c_k]\{t\}^{(e)} = [c]^{(e)}\{t\}^{(e)} \qquad (8)$$

With the help of Eq. (8), the minimization of variational integral $\chi_K^{(e)}$ is carried out, which is shown in Eq. (9):

$$\chi_K^{(e)} = \frac{1}{2}(2\pi K)\iint_A \left[[[b]^2\{t\}^{\{e\}}]^2 + [[c]^2\{t\}^{(e)}]^2\right] r dr dz \quad (9)$$

Table 3. Heat transfer parameter for four different cases of engine loading [26]

Parameter	Case 4 (Full Load)	Case 3 (3/4 Load)	Case 2 (Half Load)	Case 1 (No Load)
Temperature in °C				
T_g (Gas side)	1000	800	600	400
T_w (Water side)	120	120	120	120
T_a (Air side)	80	80	80	80
Heat transfer coefficients (Gas side, Water side, Air side) (W m^{-2} K^{-1})				
H_g (Gas side)	290.5	232.4	174.3	116.2
H_w (water side)	1859.2	1859.2	1859.2	1859.2
H_a (Air side)	174.3	174.3	174.3	174.3
Heat transfer coefficients between piston, ring and cylinder wall (W m^{-2} K^{-1})				
H_1	290.5	290.5	290.5	290.5
H_2	20.0	20.0	20.0	20.0
H_3	38346.0	38346.0	38346.0	38346.0
H_4	2324.0	2324.0	2324.0	2324.0

By simplifying the above equation and using delta operator function, Eq. (9) can be rewrite as:

$$\frac{\partial \chi_k^{(e)}}{\partial\{t\}^{(e)}} = \left(2\pi K A^{(e)} r_c\right)\left[[b]^{(e)^t}[b]^{(e)}\right] + \left[[c]^{(e)^t}[c]^{(e)}\right]\{t\}^{(e)} \quad (10)$$

where

$$\iint_A r dr dz = A^{(e)} r_c \quad r_c\,(mean\ radius) = \frac{r_i + r_j + r_k}{3}$$

Let $A^{(e)}\, r_c = V^{(e)}$; where $V^{(e)}$ is the volume of an element.

After putting the value of $[b]^{(e)}$, $[b]^{(e)t}$, $[c]^{(e)}$ and $[c]^{(e)t}$ in equation (10), generate the stiffness matrix:

$$\frac{\partial \chi_k^{(e)}}{\partial\{t\}^{(e)}} = \left(2\pi K V^{(e)}\right)\left[\begin{Bmatrix} b_i \\ b_j \\ b_k \end{Bmatrix}[b_i \quad b_j \quad b_k] + \begin{Bmatrix} c_i \\ c_j \\ c_k \end{Bmatrix}[c_i \quad c_j \quad c_k]\right]\{t\}^{(e)} \quad (11)$$

After solving the above equation, the conductive matrix becomes:

$$\frac{\partial \chi_k^{(e)}}{\partial\{t\}^{(e)}} = \begin{bmatrix} k_{11} & k_{12} & k_{13} \\ k_{21} & k_{22} & k_{23} \\ k_{31} & k_{32} & k_{33} \end{bmatrix}\begin{Bmatrix} t_i \\ t_j \\ t_k \end{Bmatrix} = [k]^{(e)}\{t\}^{(e)} \quad (12)$$

where $[k]^{(e)} = \text{stiffness matrix}$

4.2. Heat Transfer Equation for Contact Boundary

The generalized governing differential equation for contact boundary can be represented as [4]:

$$q_c = K_1\left[\frac{\partial T}{\partial n}\right]^e = -K_2\left[\frac{\partial T}{\partial n}\right]^p \quad (13)$$

where $q_c = h_c(T^e - T^p)$ (14)

Variational formulation for contact boundary between 2 elements (*e*) and (*p*) can be written as:

$$\chi_{bcont.} = \frac{h_c}{2}\int_{si}^{sj}[\{t\}^e - \{t\}^p]^2\, 2\pi r ds \quad (15)$$

Solving it further in a similar fashion as done in the conductive boundary, it was found that the contact boundary variational integral of heat transfer after differentiation, with respect to temperature of contact surface that yields a set of linear equations, to be a contribution to the global set of equation:

$$\frac{(\partial \chi_{bcont.})e}{\partial\{t_s\}^e} = \frac{2\pi h_c r_m r_{ij}}{6\cos\theta}\begin{bmatrix} 2-\frac{\varepsilon}{2} & 1 \\ 1 & 2+\frac{\varepsilon}{2} \end{bmatrix} * \begin{Bmatrix} \{\{t_s\}^e - \{t_s\}^p\}_1 \\ \{\{t_s\}^e - \{t_s\}^p\}_2 \end{Bmatrix} \quad (16)$$

4.3. Heat Transfer Equation for Convective Boundary

The generalized governing differential equation for heat convection can be represented as [4]:

$$-K\left(\frac{\partial T}{\partial n}\right) = h(T - T_\infty) \quad (17)$$

The variational formulation for convective boundary can be represented as:

$$\delta\chi_{bconv.} = \int_A -K\left(\frac{\partial T}{\partial n}\right)\delta T dS = \int_A h(T - T_\infty)\,\delta T dS \quad (18)$$

$$\delta\chi_{bconv.} = \int_i^j -Kr\left(\frac{\partial T}{\partial n}\right)\delta T dS \quad (19)$$

where, *i* and *j* are the two nodal points of the element of side *s*.

Let

$$\frac{r}{s} = cos\,\theta\,, \qquad \left(\frac{\partial T}{\partial n}\right) = h(t - t_\infty)\ and\ ds = \frac{dr}{cos\,\theta}$$

$$T(s) = N_{si}\,t_i + N_{sj}\,t_j = [N_s]\{t\} \tag{20}$$

where N_{si} and N_{sj} are the shape factor.

$$N_{si} = \frac{s_j - s}{s_{ij}} = \frac{\frac{(r_j - r)}{cos\,\theta}}{\frac{r_{ij}}{cos\,\theta}} = \frac{(r_j - r)}{r_{ij}} \tag{21}$$

$$N_{sj} = \frac{s - s_i}{s_{ij}} = \frac{\frac{(r - r_i)}{cos\,\theta}}{\frac{r_{ij}}{cos\,\theta}} = \frac{(r - r_i)}{r_{ij}} \tag{22}$$

With the help of Eqs. (20), (21) and (22), the minimization of variational integral for convective boundary can be represent as:

$$\frac{\partial \chi_{bconv.}}{\partial\{t_s\}} = \frac{2\pi h}{cos\,\theta}\int_i^j ([N_s]^T[N_s]\{t\})\,r dr - \frac{2\pi h t_\infty}{cos\,\theta}\int_i^j ([N_s]^T)\,r dr \tag{23}$$

$$\frac{\partial \chi_{bconv.}}{\partial\{t_s\}} = \frac{2\pi h r_m r_{ij}}{6cos\,\theta}\begin{bmatrix} 2-\frac{\varepsilon}{2} & 1 \\ 1 & 2+\frac{\varepsilon}{2}\end{bmatrix}\begin{Bmatrix} t_{si} \\ t_{sj}\end{Bmatrix} - \begin{Bmatrix}(ht_\infty)_1 \\ (ht_\infty)_2\end{Bmatrix} \tag{24}$$

where,

$$r_m = \frac{r_i + r_j}{2}, r_{ij} = r_j - r_i\,, r_j = r_m - \frac{r_{ij}}{2}\,, \varepsilon = \frac{r_{ij}}{r_m}$$

$$\frac{\partial \chi_{bconv.}}{\partial\{t_s\}} = [H]_s\{t\}_s - \{ht_\infty\} \tag{25}$$

5. Temperature Field Calculations

The prediction of the temperature distribution in the piston involves the solution of the heat conduction, contact and convection equation with the appropriate boundary conditions. For this purpose, the finite-element model of piston was considered. These models give satisfactory results with a significant computer time economy.

We can develop the variational integral of heat transfer globally with the help of equations (12), (16) and (25), which represent in equation (26).

$$\frac{\partial\{X\}^g}{\partial\{t\}^g} = [K]^g\{t\}^g + [H]^g\{t\}^g - \{ht_\infty\}^g = 0 \tag{26}$$

where, $\partial\{X\}^g$=Variational integral of heat transfer globally

Let

$$[K]^{(g)} + [H]^g = [D]^g$$

$$\{ht_\infty\}^{(g)} = \{V\}^{(g)}$$

Thus

$$[D]^{(g)}\{t\}^{(g)} = \{V\}^{(g)} \tag{27}$$

$$\{t\}^{(g)} = [DI]^{(g)}\{V\}^{(g)} \tag{28}$$

where

$$[DI]^{(g)} = [D]^{(g)^{-1}},\ \{t\}^{(g)} = \ global\ temperature$$

The solution of the reduced steady-state heat conduction problem in the *r*, *z* coordinate system is found through sub-dividing the piston into a number of elements and nodes. Every element exists in thermal equilibrium with its neighboring elements. After formulating the heat transfer equations, a computational code to solve the mathematical model through FORTRAN language is generated, and the temperature at all the nodes is found. Then the temperature field (isothermal distribution curve) in the diesel engine piston model is obtained.

6. Discussion of Results

As results indicate, the thermal energy is much more utilized to generate work output due to air cavity. It reduces the weight and cost of the piston because the cost associated with thermal barrier coating is reduced on the piston crown. This new method should be supported by research comprising the application of thermodynamic principles and the fundamental equations of heat transfer. Here, the finite element analysis is used to obtain temperature at all the nodal points. The results of calculations carried out are presented in Figures 3-7. Figures 3-6 show the temperature field (isothermal distribution) and Figure 7 shows the heat flow rate through the piston under four different engine thermal loading conditions having gas temperatures of 1000°C, 800°C, 600°C and 400°, respectively, with and without air cavity. The continuous lines show the temperature field and the heat flow rate for conventional piston, while the dotted lines show the temperature field and the heat flow rate for the case when there is an air cavity inside the piston. The maximum and minimum temperature values are determined as 449°C and 110°C at the top and bottom surface of conventional piston bowl, respectively. And in air cavity piston, the maximum and minimum temperature values are determined as 464°C and 111°C at the top and bottom surface of the piston bowl, as shown in Table 4. Movement of the maximum temperature from the piston top surface to the bottom surface of the piston is attributed to the fact that the top surface has a relatively larger heat transfer coefficient as compared to the bottom surface. Since the inner side surface of the piston was voided circumferentially with a relatively very low conduction coefficient material, i.e., air, so heat transfer was reduced considerably to it. Therefore, the top surface temperature, as observed, was high as compared to the conventional piston. The maximum surface temperature of the base metal of the cavity piston is seen to be 464°C. It, as shown, increases the combustion chamber temperature of the engine. The comparison shows that there is a tendency to decrease the heat flow rate in the air cavity piston body.

To check the validity of the heat transfer model, the heat balance approached was adopted. According to the principle of the conversion of energy, at a steady state condition, the heat entering to the piston from gas side is equal to the heat lost to water and air. It was found that the temperature, at all the nodal points, was accurate as they are satisfying heat flow boundary conditions. Hence, the results are meaningful. Initially, the piston was heated at a

much higher rate, as the temperature was less. Gradually, the temperature increases and as a result of this the heat input to it decreases till the steady state condition is reached as shown in Figure 7. Figure 7 shows the variation in heat gain by the piston from hot gases 'Qg', heat lost to cooling water 'Qw' and heat lost to air 'Qa' under four different engine thermal loading conditions, for both cases with and without air cavity in the diesel piston. It seems that piston received the heat from hot gases, which increases with the increase in the engine loads. Similarly, the heat lost to water, and heat lost to air, also increases with the increase in engine loads, as shown in Table 5. In Figure 7, it can be observed that the error is very small between the heat supplied (Qg) by the combustion gasses and the heat rejected to water (Hw) and air sides (Ha). It represents a uniform percentage throughout all the tests. As expected, for steady state conditions, the heat transfer rate increases with engine loading condition, with a maximum observed at full load. Here, in the present analysis, the heat balance equation is satisfied for all the different loading conditions. So it presumed that the obtained temperature field and heat flow rate are accurate as they are satisfying heat flow boundary conditions. Hence, the results are meaningful. The influence of air cavity is shown by the fact that the temperature variation in the piston is reduced by the application of this cavity. Hence, the air cavity plays an important role in reducing the temperature levels of the piston and, thus, reduces the thermal stresses, reduces the heat loss through the piston and improves the work output.

Table 4. Maximum and minimum temperature in the engine piston

	Conventional Piston		Air-cavity piston	
	Max. Temp. (°C)	Min. Temp. (°C)	Max. Temp. (°C)	Min. Temp. (°C)
Case 1 (No Load)	463.769	111.227	449.689	111.288
Case 2 (Half Load)	345.378	110.760	335.352	110.798
Case 3 (3/4 Load)	261.291	110.434	254.831	110.459
Case 4 (Full Load)	188.850	110.155	185.738	110.170

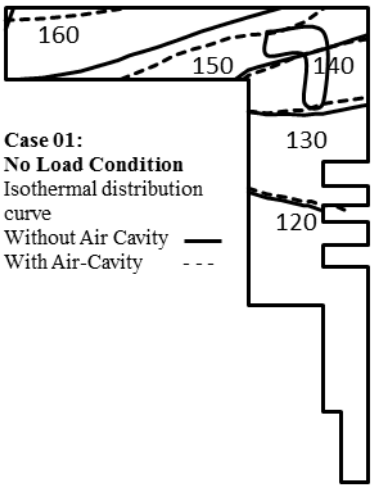

Figure 3. Temperature field at no load

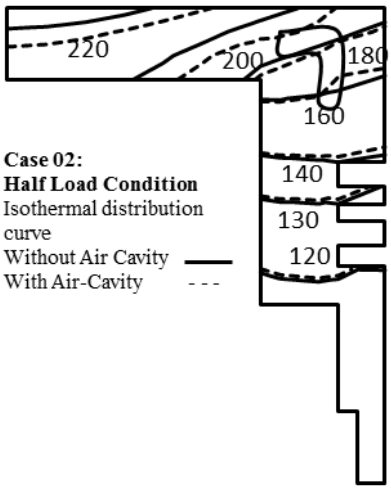

Figure 4. Temperature field at 1/2 load

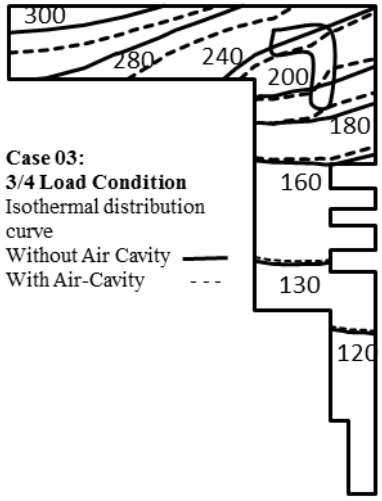

Figure 5. Temperature field at 3/4 load

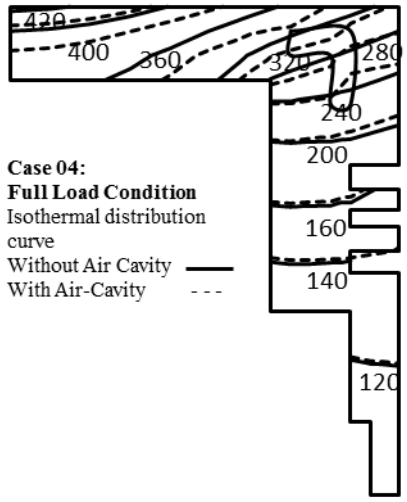

Figure 6. Temperature field at full load

Table 5. heat flow rates through piston with gas temperature

Heat Flow rate (kW/Hr)	Conventional Piston (Without air cavity)				Air-cavity piston			
	No Load	Half Load	3/4 Load	Full Load	No Load	Half Load	3/4 Load	Full Load
Q_g	5.094	9.797	15.341	23.417	5.298	10.179	15.924	24.354
Q_a	2.605	3.282	4.072	5.198	2.708	3.407	4.231	5.406
Q_w	2.489	6.515	11.268	18.219	2.588	6.762	11.707	18.945

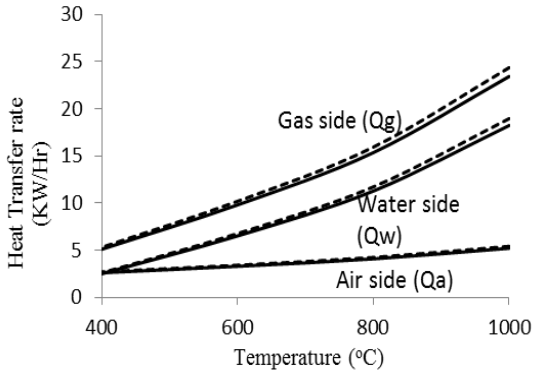

Figure 7. Variation of the heat flow rates through piston with gas temperature

7. Conclusion

The present study indicates that an air cavity applied in the piston has the following effects:

- It decreases the overall body temperature of the piston. The values of temperature and thus thermal stress will further decrease by increasing the cavity thickness up to a certain limit.
- By the application of this cavity in the piston, the reduction in heat loss through the piston is found to be nearly 4%. The percentage distribution of heat loss through cooling media remains unaffected at low loads while it is significantly affected at high loads.

The temperature and heat transfer are obtained by indirect evaluation of the boundary conditions of the piston. The variational integral method in FEM presented here may be used for other parts of I.C. engines, such as the inlet and exhaust valves, cylinder heads, etc. This method is a powerful tool for the design engineer when used in the early stages of the design of a semi-adiabatic engine. In development work, it enables the development engineer to narrow the range of the experimental work and thus save considerable time and expense.

References

[1] H. Yasar, H.S. Soyhan, H. Walmsley, B. Head, C. Sorusbay, "Double-Wiebe function: an approach for single-zone HCCI engine modeling". Applied Thermal Engineering, Vol. 28 (2008), 1284-1290.

[2] R. Stone, "Introduction to Internal Combustion Engines". New York: Macmillan; 1999.

[3] C. F. Taylor, T. Y. Toong, "Heat transfer in internal-combustion engines". ASME paper 57-HT-17 (1957).

[4] G. A. Woschni, "Universally applicable equation for the instantaneous heat transfer coefficient in the internal combustion engine". SAE 670931 (1967).

[5] G. F. Hohenberg, "Advanced approaches for heat transfer calculation". SAE 790825 (1979).

[6] J. Chang, O. Guralp, Z. Filipi, D. Assanis, T. Kuo, P. Najt, R. Rask, "New heat transfer correlation for an HCCI engine derived from measurements of instantaneous surface heat flux". SAE 2004-01-2996 (2004).

[7] G. Borman, K. Nishiwaki, "Internal combustion engine heat transfer". Progress in Energy and Combustion Science, Vol. 13 (1987) No. 1, 1-46.

[8] P. Tamilporai, N. Baluswamy, P.M. Jawahar, S. Subramaniyam, S. Chandrasekaran, K. Vijayan, S. Jaichandar, J. R. Janci, K. Arunachalam, "Simulation and analysis of combustion and heat transfer in low heat rejection diesel engine using two zone combustion model and different heat transfer models". SAE 2003-01-1067 (2003).

[9] V. Esfahanian, A. Javheri, M. Ghaffarpour, "Thermal analysis of an SI engine piston using different combustion boundary condition treatments". Applied Thermal Engineering, Vol. 26 (2006), 277-287.

[10] A. Jafari, S. K. Hannani, "Effect of fuel and engine operational characteristics on the heat loss from combustion chamber surfaces of SI engines". International Communications in Heat and Mass Transfer, Vol. 33 (2006) No. 1, 122-134.

[11] I. Taymaz, "An analysis of residual stresses in thermal barrier coatings: a FE performance assessment". Plasma Processes and Polymers, Vol. 6 (2009), 599-604.

[12] E. Buyukkaya, M. Cerit, "Thermal analysis of a ceramic coating diesel engine piston using 3-D finite element method". Surface and Coatings Technology, Vol. 202 (2007) No. 2, 398-402.

[13] E. Abu-Nada, I. Al-Hinti, A. Al-Sarkhi, B. Akash, "Thermodynamic modeling of spark-ignition engine: Effect of temperature dependent specific heats". International Communication in Heat and Mass Transfer, Vol. 33 (2006), 1264–1272.

[14] R. Soltani, H. Samadi, E. Garcia, T. W. Coyle, "Development of alternative thermal barrier coatings for diesel engines". SAE International, Vol. 01 (2005), 65-72.

[15] J. B. Heywood, "Internal Combustion Engine Fundamentals". McGraw-Hill Inc New York, 1988.

[16] C. D. Rakopoulos, K. A. Antonopoulos, D. C. Rakopoulos, E. G. Giakoumis, "Investigation of the temperature oscillations in the cylinder walls of a diesel engine with special reference to the limited cooled case". International Journal of Energy Research, Vol. 28 (2004), 977–1002.

[17] Ravindra Prasad and N. K. Samria, "Transient Heat Transfer Studies on a diesel engine valve". International Journal of Mechanical Science, Vol. 33 (1991), 179-195.

[18] David R. Buttsworth, A. Agrira, R. Malpress, T. Yusaf, "Simulation of instantaneous heat transfer in spark ignition internal combustion engines: Unsteady thermal boundary layer modeling". Journal of Engineering for Gas Turbines and Power, Vol. 133 (2011), 45-56.

[19] A. Mohammadi, M. Yaghoubi, "Estimation of instantaneous heat transfer coefficient in spark-ignition engines". International Journal of Thermal Science, Vol. 49 (2010), 1309-1317.

[20] T. T. Mon, R. Mamat, Kamsah Nazri, "Thermal analysis of SI Engine using simplified finite element model". World Congress on Engineering, London, U.K., Vol. 3 (2011), 66-71.

[21] B. Zhao, "Thermal stress analysis of ceramic coated diesel engine piston based on the wavelet finite element method". Journal of Engineering Mechanics, Vol. 138 (2012), 166-172.

[22] A. Al-Sarkhi, B. Akash, E. Abu-Nada, and I. Al-Hinti, "Efficiency of Atkinson Engine at Maximum Power Density using Temperature Dependent Specific Heats". Jordan Journal of Mechanical and Industrial Engineering, Vol. 2 (2008), 71-75.

[23] Muhammet Cerit, "Thermo mechanical analysis of a partially ceramic coated piston used in an SI engine". Surface Coating & Technology, Vol. 205 (2011), 3499–3505.

[24] Tyler R. Kakuda, Andi M. Limarga, T. D. Bennett and David R. Clarke, "Evolution of thermal properties of EB-PVD 7YSZ thermal barrier coating with thermal cycling". Acta Material, Vol. 57 (2009), 2583-2591.

[25] K. R. Vijaya Kumar, V. Sundareswaran, "The Effect of Thermal Barrier Coatings on Diesel Engine Performance of PZT Loaded Cyanate Modified Epoxy Coated Combustion Chamber". Jordan Journal of Mechanical and Industrial Engineering, Vol. 5 (2011) No. 5, 403-406.

[26] S. K. Sharma, P. K. Saini, N. K. Samria, "Experimental thermal analysis of diesel engine piston and cylinder wall". Journal of engineering, Article ID 178652 (2015), 1- 10.

[27] Ravindra Prasad, N. K. Samria, "Heat transfer and stress fields in the inlet and exhaust valve of a semi-adiabatic diesel engine". Computer Structure, Vol. 34 (1990), 165-711.

[28] V. P. Singh, P. C. Upadhyay, N. K. Samria, "Some heat transfer studies on a diesel engine piston". International Journal of Heat & Mass Transfer, Vol. 29 (1986), 812-814.

[29] Ravindra Prasad, N. K. Samria, "Transient heat transfer analysis an internal combustion engine piston". Computer Structure, Vol. 34 (1990), 781-193.

[30] S. K. Sharma, P. K. Saini, N. K. Samria, "Modelling and analysis of radial thermal stresses and temperature field in diesel engine valves with and without air cavity". International Journal of Engineering, Science and Technology, Vol. 5 (2013) No. 3, 111-123.